Freezing of QCD coupling affects the short distance static potential

A. M. Badalian* and D. S. Kuzmenko†
Institute of Theoretical and Experimental Physics, 117218, B. Cheremushkinskaya 25, Moscow, Russia
(Received 5 June 2001; published 11 December 2001)

A striking contradiction between the lattice short-range static potential ($n_f=0$) and standard perturbative potential is investigated in the framework of the background perturbation theory. With the use of the background coupling $\tilde{\alpha}_B(r)$ which contains the only background parameter, the mass m_B, fixed by the fine-structure fit in bottomonium, the lattice data are nicely explained without the introduction of an exotic short-range linear potential with a large "string tension" $\sigma^* \sim 1$ GeV^2. A significant difference between $\tilde{\alpha}_B(r)$ and standard perturbative strong coupling $\alpha_V(r)$ is found in the range 0.05 fm $\lesssim r \lesssim 0.15$ fm, while at larger distances, $r>0.3$ fm, $\tilde{\alpha}_B(r)$ fast approaches the freezing value $\tilde{\alpha}_B(\infty)$. Some problems concerning the strong-coupling properties at short and long distances are discussed and solutions are suggested.

DOI: 10.1103/PhysRevD.65.016004 PACS number(s): 11.15.Bt, 12.38.Lg

I. INTRODUCTION

The property of the freezing of the strong coupling constant $\tilde{\alpha}_V(r)$ at long distances is widely used in QCD phenomenology [1–6]. On a fundamental level this phenomenon has been studied in two different theoretical approaches [7–9]. In the case of the static potential, the freezing of the coupling $\tilde{\alpha}_V(r)$ suggests that $\tilde{\alpha}_V(r)$ is approaching a constant $\alpha_{\rm fr} \equiv \tilde{\alpha}_V(r \to \infty)$ at relatively long distances while at small r it manifests the property of asymptotic freedom. Both characteristic features of the static potential were widely used in hadron spectroscopy. However, it was realized that the asymptotic freedom behavior does not practically affect hadron spectra, being important mostly for a wave function at the origin. On the contrary, the choice of $\tilde{\alpha}_V(r)$ as a constant at all distances, i.e., $\tilde{\alpha}_V(r) \cong \bar{\alpha}$, appears to be a reasonable approximation and gives rise to a good description of meson spectra both for heavy quarkonia [1,10,11] and for heavy-light mesons [12]. Also in lattice QCD this choice gives a good fit to the lattice static potential at distances above 0.2 fm.

Therefore, the question arises why this simple approximation, $\tilde{\alpha}_V(r) \approx \bar{\alpha}$, works so well even in the case of bottomonium where the sizes of low-lying levels are not large, the characteristic radius $R_{\rm ch} \lesssim 0.5$ fm. To answer this question one needs to clarify another problem, namely to find out the precise freezing value of the vector constant in momentum and coordinate spaces, and to define the distances r where the difference between $\tilde{\alpha}_V(r)$ and $\alpha_{\rm fr}$ is becoming inessential and therefore the approximation $\tilde{\alpha}_V(r) = \bar{\alpha}$ ($\bar{\alpha} \neq \alpha_{\rm fr}$ in the general case) gives a good description of hadron spectra and other physical characteristics.

This problem will be discussed in the present paper in the framework of background perturbation theory (BPT) and it will be shown that the background coupling $\tilde{\alpha}_B(r)$ approaches its freezing value already at rather small distances $r>0.4$ fm. Here it is worthwhile to remember that in most calculations in coordinate space the "average" value $\bar{\alpha}$ is usually taken in the range $0.35 \lesssim \bar{\alpha} \lesssim 0.45$ while in momentum space larger critical values were used [$\alpha_{\rm cr} \equiv \alpha_V(q=0)$]. For example, in Ref. [3] $\alpha_{\rm cr}=0.60$ and for the Richardson potential $\alpha_{\rm cr}=2\pi/\beta_0 \approx 0.7$ ($n_f=3$) [2,13], i.e., the difference between $\alpha_{\rm cr} \approx 0.6-0.7$ in momentum space and $\bar{\alpha} \approx 0.40 \pm 0.05$ in coordinate space is essential. However, this difference was not confirmed by the analysis of the QCD coupling in background fields [14] where the vector coupling constants $\alpha_B(q)$ and $\tilde{\alpha}_B(r)$ were found to have the same asymptotic value:

$$\alpha_B(q=0) = \tilde{\alpha}_B(r \to \infty) = \alpha_{\rm fr}. \tag{1}$$

This equality takes place also for the phenomenological coupling taken as a sum of Gaussians in Ref. [3].

In lattice measurements of the static potential at long distances, the freezing phenomenon is also seen, however existing lattice data have not clarified our knowledge about $\alpha_{\rm fr}$. As shown in Refs. [15,16] the lattice static potential at $r \geqslant 0.2$ fm can be parametrized with good accuracy by the Cornell potential with rather small $\bar{\alpha}$ (in lattice notation $\frac{4}{3}\bar{\alpha} = e$). In the quenched approximation ($n_f=0$), the fitted lattice values of $\bar{\alpha} \approx 0.20-0.24$ ($e=0.27-0.32$) turned out to be small so that in some cases there appears to be a discontinuity of the vector coupling constant at the matching point, $r_{\rm mat} \approx 0.2$ fm [5]. But if dynamical fermions are introduced, in lattice QCD the fitted value of $\bar{\alpha}(n_f=2,3)$ was found to become larger, $\bar{\alpha} \cong 0.30$ ($e \cong 0.40$) [17] still being less than in phenomenological models.

Another problem concerns the behavior of $\tilde{\alpha}_V(r)$ at short distances. The most interesting and unexpected results were obtained in lattice measurements of the static potential at short distances, 0.05 fm $\leqslant r \leqslant 0.15$ fm [18], where a large difference between the lattice and the two-loop (one-loop) perturbative potential was observed, yielding a discrepancy of about 100% at the point $r=0.15$ fm. In Ref. [18], this

*Email address: badalian@heron.itep.ru
†Email address: kuzmenko@heron.itep.ru

large difference was parametrized by a short distance linear term $\sigma^* r$ with the slope $\sigma^* \approx 1$ GeV^2.

This effect will be explained in our paper. To this end the strong- coupling constant in background fields $\tilde{\alpha}_B(r)$ will be calculated and the influence of the background mass m_B will be shown to become essential already at rather short distances. We have found that there is no need to introduce an additional exotic linear potential $\sigma^* r$ as in Ref. [18]. The resulting static potential $V_B(r)$ appears to have an effectively linear term in good agreement with lattice data. In our calculations no fitting parameters are introduced: the value of the background mass $m_B = 1.0$ GeV is taken from fine-structure analysis in bottomonium [11] while the QCD constant $\Lambda_{\overline{MS}}(n_f = 0)$ is considered as a well established number and taken from Ref. [19].

II. THE STRONG-COUPLING CONSTANT $\alpha_B(q)$ IN BACKGROUND FIELD THEORY

The perturbative static potential is used to define a coupling constant $\alpha_V(q)$ in V-scheme:

$$V_P(q) = -4\pi C_F \frac{\alpha_V(q)}{q^2}, \tag{2}$$

where $q^2 \equiv \mathbf{q}^2$. Recently the renormalized $\alpha_V(q)$ was calculated in the two-loop approximation [20,21]. In coordinate space the static potential can be defined as the Fourier transform of $V_P(q)$,

$$V_P(r) = \int \frac{d\mathbf{q}}{(2\pi)^3} V_P(q) \exp(i\mathbf{qr}), \tag{3}$$

which gives rise to the simple relation between the coupling constants:

$$\tilde{\alpha}_V(r) = \frac{2}{\pi} \int_0^\infty dq \frac{\sin qr}{q} \alpha_V(q), \tag{4}$$

if the following definition for the coupling in coordinate space $\tilde{\alpha}_V(r)$ is used:

$$V_P(r) = -C_F \frac{\tilde{\alpha}_V(r)}{r}. \tag{5}$$

However, the Fourier transform of the perturbative coupling $\alpha_V(q)$, Eq. (4), does not exist in a strict sense because of Landau pole singularity. To escape IR divergency the expansion of $\alpha_V(q)$ in the perturbative series at large q^2 is usually made [20,21], but the resulting expansion is valid only at short distances.

Here we suggest to obtain the static potential in coordinate space with the use of the coupling in BPT, where the vector coupling constant $\alpha_B(q)$ in momentum space is defined at all momenta and has no singularity for $q^2 > 0$ [7]. Then the potential in momentum space can be written as in Eq. (2),

$$V_B(q) = -C_F 4\pi \frac{\alpha_B(q)}{q^2}. \tag{6}$$

In Eq. (6) and below we consider the influence of background vacuum fields only on Coulomb-type interaction. In the presence of background fields the QCD coupling is modified so that it depends on the combination $(q^2 + m_B^2)$ instead of q^2 as it is in standard perturbative theory [8]. The mass m_B is a background mass which is characteristic for a process considered. In the two-loop approximation the running background coupling is

$$\alpha_B^{(2)}(q) = \alpha_B^{(1)}(q) \left\{ 1 - \frac{\beta_1}{\beta_0^2} \frac{\ln t_B}{t_B} \right\}, \tag{7}$$

where the one-loop expression is given by

$$\alpha_B^{(1)}(q) = \frac{4\pi}{\beta_0 t_B}, \tag{8}$$

with

$$t_B = \ln \frac{q^2 + m_B^2}{\Lambda_V^2}. \tag{9}$$

The condition $m_B > \Lambda_V$ is assumed to be satisfied under the logarithm (9) to guarantee the absence of the Landau pole; this condition is always valid for the numbers Λ_V and m_B used in our calculations [see the numbers in Eq. (25)].

In Eq. (7),

$$\beta_0 = 11 - \frac{2}{3} n_f, \quad \beta_1 = 102 - \frac{38}{3} n_f. \tag{10}$$

First we discuss the most important properties of the background coupling $\alpha_B(q)$.

The background mass m_B is not an arbitrary parameter. It can be calculated in the framework of BPT or in lattice QCD. As was shown in Ref. [22], the background mass m_B in the case of the static potential is defined by the difference of two-gluon and one-gluon hybrid excitations and can be extracted from the corresponding level differences of hybrids $c\bar{c}g, b\bar{b}g$. In Ref. [22], this mass m_B was evaluated to be 1.0–1.2 GeV. For other processes, such as $e^+e^- \to$hadrons, in general the background mass m_B may be different [8]. The appearence of the mass m_B in Eq. (9) is similar to the case of QED where α has the mass of an e^+e^- pair under logarithm.

It is of interest to notice that the analytical form of $\alpha_B(q)$ (7) coincides with that obtained in a picture when a gluon is supposed to have an effective mass m_g inside the gluon loop. Therefore, in Ref. [23] $\alpha_s(q)$ was taken as a function of $(q^2 + 4m_g^2)$, i.e., the double effective gluon mass $2m_g$ plays a role of the background mass m_B (see the discussion in Ref. [4]).

In our calculations here the value of m_B will be fixed at $m_B = 1.0$ GeV, taken from the fit to fine-structure splittings in bottomonium [11].

At large momenta, $q^2 \gg m_B^2$, the background coupling goes over into the standard perturbative expression $\alpha_V(q)$. Therefore, the QCD constants $\Lambda_{\overline{\rm MS}}$ in PQCD and $\Lambda^B_{\overline{\rm MS}}$ in BPT must coincide; in any case it is true for the number of flavors $n_f=5$. As can be directly calculated with the use of the matching procedure, they are also equal for $n_f=4$.

The QCD constant Λ_V, entering the coupling $\alpha_V(q)$ in Eq. (2), can be expressed through $\Lambda_{\overline{\rm MS}}(n_f)$ in the modified minimal subtraction ($\overline{\rm MS}$) renormalization scheme [24]:

$$\Lambda_V^{(n_f)} = \Lambda_{\overline{\rm MS}}^{(n_f)} \exp\left(\frac{a_1}{2\beta_0}\right), \tag{11}$$

with

$$a_1 = \frac{31}{3} - \frac{10}{9} n_f. \tag{12}$$

At present the values of $\Lambda_{\overline{\rm MS}}^{(n_f)}$ are well established for the number of flavors $n_f=5$: $\Lambda_{\overline{\rm MS}}^{(5)} = 208 \pm^{25}_{23}$ MeV [25] and also for $n_f=0$ due to an analysis in the lattice finite size technique [19]:

$$\Lambda_{\overline{\rm MS}}^{(0)} = \frac{602(48)}{r_0}, \tag{13}$$

where r_0 denotes the Sommer scale. With the use of $r_0 = 2.5\ \ {\rm GeV}^{-1}$, taken in most lattice calculations [17,18], one obtains

$$\Lambda_{\overline{\rm MS}}^{(0)} = 241 \pm 19\ \ {\rm MeV}. \tag{14}$$

Then from Eq. (11) the QCD constant in the V-scheme is

$$\Lambda_V^{(0)} = 385 \pm 30\ \ {\rm MeV}. \tag{15}$$

In the three-loop approximation the background coupling

$$\alpha_B^{(3)}(q) = \alpha_B^{(1)}(q)\left\{1 - \frac{\beta_1}{\beta_0^2}\frac{\ln t_B}{t_B} + \frac{\beta_1^2}{\beta_0^4 t_B^2}\left[(\ln t_B)^2 - \ln t_B - 1 + \frac{\beta_2^V \beta_0}{\beta_1^2}\right]\right\} \tag{16}$$

contains the term including the β_2^V coefficient, which depends on a renormalization scheme and was calculated in Refs. [20,21] (the coefficients β_0, β_1 do not depend on the renormalization scheme); this coefficient

$$\beta_2^V = \beta_2^{\overline{\rm MS}} - a_1\beta_1 + (a_2 - a_1^2)\beta_0. \tag{17}$$

Here a_1 is defined by Eq. (12) and

$$\beta_2^{\overline{\rm MS}} = \frac{2857}{2} - \frac{5033}{18} n_f + \frac{325}{54} n_f^2, \tag{18}$$

$$a_2 = 9\left(\frac{4343}{162} + 4\pi^2 - \frac{\pi^4}{4} + \frac{22}{3}\zeta(3)\right) + \frac{100}{81} n_f^2 - \frac{3}{2} n_f \left(\frac{1798}{81} + \frac{56}{3}\zeta(3)\right) - \frac{2}{3} n_f \left(\frac{55}{3} - 16\zeta(3)\right). \tag{19}$$

In Eq. (19), $\zeta(3) = 1.202057$ denotes the Riemann ζ function. In the quenched approximation,

$$a_2(n_f=0) = 456{,}7488, \qquad \beta_2^V(n_f=0) = 4224{,}1817, \tag{20}$$

i.e., the β_2^V coefficient turns out to be about three times larger than $\beta_2^{\overline{\rm MS}}(n_f=0) = \frac{2857}{2}$. As a result, the third-order correction in $\alpha_B^{(3)}(q)$ is much larger than $\alpha_B^{(1)}(q)$ and $\alpha_B^{(2)}(q)$.

It is easy to find the first-order correction to the perturbative coupling $\alpha_V(q)$ which comes from the expansion of $\alpha_B(q)$ in powers of m_B^2/q^2. In the two-loop approximation,

$$\alpha^{(2)}_{\rm appr}({\rm large}\ \ q) = \alpha_V^{(2)}(q) - \alpha_V^{(1)}(q)\frac{m_B^2}{q^2 \ln \dfrac{q^2}{\Lambda_V^2}}, \tag{21}$$

with

$$\alpha_V^{(2)}(q) = \alpha_V^{(1)}(q)\left(1 - \frac{\beta_1}{\beta_0^2}\frac{\ln y}{y}\right), \quad \alpha_V^{(1)}(q) = \frac{4\pi}{\beta_0 y}, \qquad y = \ln\frac{q^2}{\Lambda_V^2}. \tag{22}$$

This approximation appears to be valid only at $q > 2$ GeV (with an accuracy $\lesssim 10\%$).

The behavior of $\alpha_B(q)$ in the IR region. The freezing value of $\alpha_B^{(n)}(q)$ can be easily obtained from Eqs. (7)–(9), in particular for two-loop coupling,

$$\alpha_{\rm cr}^{(2)} = \alpha_B^{(2)}(q^2=0) = \frac{4\pi}{\beta_0 t_0}\left\{1 - \frac{\beta_1}{\beta_0^2}\frac{\ln t_0}{t_0}\right\} \tag{23}$$

with

$$\alpha_{\rm cr}^{(1)} = \frac{4\pi}{\beta_0 t_0}; \quad t_0 = t_B(q^2=0) = \ln\frac{m_B^2}{\Lambda_V^2}. \tag{24}$$

In what follows, the notation $\alpha_{\rm cr}^{(n)} = \alpha_B^{(n)}(q^2=0)$, as in potential models [3], is also used. The parameters m_B and Λ_V, present in t_B, are considered to be fixed: the value of m_B is taken from fine-structure analysis of $2P$ and $1P$ states in bottomonium while the value $\Lambda_V^{(0)}(n_f=0)$ is taken from lattice data and given by Eq. (15),

$$m_B = 1.0\ \ {\rm GeV}, \quad \Lambda_V^{(0)}(n_f=0) = 385\ \ {\rm MeV}. \tag{25}$$

We suppose here that for $n_f=3$ the constants $\Lambda_V^{(3)}$ and $\Lambda_V^{(0)}$ are approximately equal,

$$\Lambda_V(n_f=3)\simeq\Lambda_V(n_f=0)=385\pm30 \ \text{MeV}. \tag{26}$$

Then the following critical values can be obtained from Eqs. (7) and (15):

$$\alpha_{\rm cr}^{(1)}=0.598; \quad \alpha_{\rm cr}^{(2)}=0.428; \quad \alpha_{\rm cr}^{(3)}=0.805 \quad (n_f=0), \tag{27}$$

$$\alpha_{\rm cr}^{(1)}=0.731; \quad \alpha_{\rm cr}^{(2)}=0.536; \quad \alpha_{\rm cr}^{(3)}=0.972 \quad (n_f=3). \tag{28}$$

As one can see from Eqs. (27) and (28), the third-order coupling turns out to be about 90% ($n_f=0$) and 80% ($n_f=3$) larger than $\alpha_{\rm cr}^{(2)}(n_f)$ because of large β_2^V coefficient (20). Such a value of $\alpha_{\rm cr}^{(3)}(n_f)$ appears to be too large and not compatible with the effective Coulomb constant of the static potential, $\alpha_{\rm eff}\lesssim0.5$, needed to describe heavy quarkonia [1,3] and heavy-light meson spectra [12]. Such a large value of the Coulomb constant is also not observed in lattice calculations of the static potential at large distances [15,16].

Presumably this means that since the perturbative series is an asymptotic one, it should be truncated after the second-loop term.

Recently an ''analytical'' perturbation theory was elaborated in [9]. It was shown there that the modification of singularities of perturbative coupling by power terms allows us to work accurately in the two-loop approximation. The third-order contribution becomes numerically inessential and, e.g., for e^+e^- annihilation is about 0.5%.

Therefore, in what follows the third-order term will be omitted and *a posteriori* our phenomenological analysis with the use of background coupling will demonstrate that the two-loop approximation is sufficient to describe the lattice data at small distances.

The background coupling $\alpha_B^{(2)}(q)$ in the two-loop approximation turns out to be rather close to the phenomenological $\alpha_{\rm ph}(q)$ which is successfully used in hadron spectroscopy. For comparison, $\alpha_{\rm ph}(q)$ will be taken from the well-known paper of Godfrey and Isgur [3]:

$$\alpha_{\rm GI}=0.25\exp(-q^2)+0.15\exp(-0.1q^2)+0.20\exp(-0.001q^2) \tag{29}$$

with q in GeV and $\alpha_{\rm cr}=0.60$.

In Fig. 1, this phenomenological coupling is compared to the background coupling $\alpha_B^{(2)}(q)$ for $n_f=3$. Here, as in Eq. (26), it is supposed that $\Lambda_V(n_f=3)\cong\Lambda_V(n_f=0)$ and for $\Lambda_V(n_f=3)$ two values are taken:

$$\text{(a)} \ \ \Lambda_V(n_f=3)=385 \ \text{MeV}, \qquad \text{(b)} \ \ \Lambda_V(n_f=3)=410 \ \text{MeV}. \tag{30}$$

These values of $\Lambda_V^{(3)}$ do not contradict those which are commonly used in the $\overline{\rm MS}$ renormalization scheme, and give rise to $\alpha_s(M_Z)=0.118\pm0.001$. The connection between $\Lambda_{\overline{\rm MS}}^{(n_f)}$ and $\Lambda_V^{(n_f)}$ is given by Eq. (11).

In Fig. 1, the couplings $\alpha_{\rm GI}(q)$ (solid line), $\alpha_B^{(2)}(q)$ in the two-loop approximation with $\Lambda_V=385$ MeV (dashed line), and $\alpha_B^{(2)}(q)$ with $\Lambda_V=410$ MeV (dash-dotted line) and $m_B=1.0$ GeV are shown. At the momentum $q=\overline{m}_c=1.3$ GeV ($\overline{m}_c$ is the running mass of the c quark), the matching of the couplings was done with the following result for the QCD constant: $\Lambda_V(n_f=4)=0.325$ MeV in the case (a) and $\Lambda_V(n_f=4)=351$ MeV in the case (b). As is seen from Fig. 1, the background coupling $\alpha_B^{(2)}(q)$ in the case (b) [and to some extent in case (a)] appears to be very close to the phenomenological coupling $\alpha_{\rm GI}(q)$; the difference between them is less than 5% at small $q\lesssim1.3$ GeV and less than 2% in the range $1.3\leqslant q\leqslant4$ GeV. So one can expect that with the use of the background coupling, an equally good description of low-energy experimental data can be obtained as in Ref. [3] with the use of the phenomenological coupling. From here our estimate of the freezing value is about $0.53-0.60$, and it is interesting to look at the expansion of the background coupling $\alpha_B(q)$ near the freezing point $q=0$:

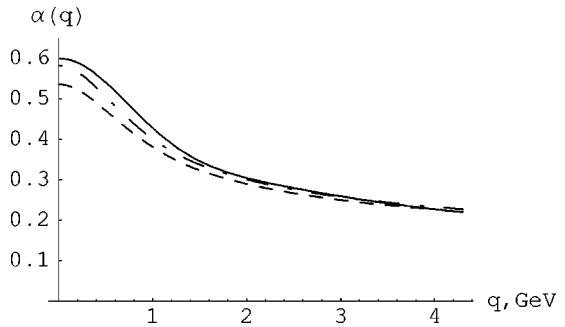

FIG. 1. The behavior of the background coupling $\alpha_B^{(2)}(q)$ for $\Lambda_V^{(3)}=385$ MeV (dashed line) and for $\Lambda_V^{(3)}=410$ MeV (dash-dotted line) compared to the phenomenological coupling $\alpha_{\rm GI}(q)$ (solid line) taken from Ref. [3].

$$\alpha_{\rm appr}^{(2)}(\text{small } q)=\alpha_{\rm cr}^{(2)}-\alpha_{\rm cr}^{(1)}\frac{q^2}{m_B^2\ln\dfrac{m_B^2}{\Lambda_V^2}}, \tag{31}$$

where $\alpha_{\rm cr}^{(2)},\alpha_{\rm cr}^{(1)}$ are the fixed numbers defined by m_B and Λ_V [see Eqs. (23) and (24)]. This approximation appears to be valid only in a very narrow range of small momenta q, $0\leqslant q\leqslant0.4$ GeV, where the difference between $\alpha_B^{(2)}(q)$ and $\alpha_{\rm appr}^{(2)}$ (small q) is less than 5%; but it already reaches 22% at $q=1.0$ GeV.

Heavy-quark initiated jets can be successfully described at small momenta if the following assumption is made about an effective coupling constant $\alpha_{\rm eff}(q)$ in the infrared region [6]:

$$J_2(\text{fit})=(2 \ \text{GeV})^{-1}\int_0^{2 \ \text{GeV}}dq\frac{\alpha_{\rm eff}(q)}{\pi}=0.18\pm0.01(\text{exp})\pm0.02(\text{th}). \tag{32}$$

As was shown in Ref. [6], this number does not depend on the form of $\alpha_{\rm eff}(q)$ assumed in the fit. Our calculations of the

integral (32) with the background coupling $\alpha_B^{(2)}(q)$ from Eq. (7) with $n_f=3$, $\Lambda_V=410$ MeV, and $m_B=1.0$ GeV give

$$J_2(\alpha_B)=(2\ \text{GeV})^{-1}\int_0^{2\ \text{GeV}}\frac{dq}{\pi}\alpha_B^{(2)}(q)=0.134, \quad (33)$$

i.e., this number is 26% smaller than J_2(fit) in Eq. (32). The same integral calculated with the phenomenological constant $\alpha_{\rm GI}(q)$ (29) is also 22% smaller than J_2(fit) (the central value):

$$J_2(\alpha_{\rm GI})=0.14 \quad (34)$$

and very close to our number (33). One should notice here that the large number (32) in Ref. [6] could be connected with the large fitted value of $\alpha_s^{\overline{\rm MS}}(M_Z)=0.125\pm0.003(\text{exp})=0.004(\text{th})$, used in their paper, while now the average $\alpha_s^{\overline{\rm MS}}(M_Z)=0.118\pm0.001$ is accepted [25,26].

In conclusion we give our predictions about the freezing values in momentum space:

$$\alpha_{\rm cr}^{(1)}=0.598, \quad \alpha_{\rm cr}^{(2)}=0.428 \quad (n_f=0, \quad \Lambda_V^{(0)}=385\ \text{MeV}),$$
$$\alpha_{\rm cr}^{(1)}=0.731, \quad \alpha_{\rm cr}^{(2)}=0.536 \quad (n_f=3, \quad \Lambda_V^{(3)}=385\ \text{MeV}), \quad (35)$$
$$\alpha_{\rm cr}^{(1)}=0.783, \quad \alpha_{\rm cr}^{(2)}=0.582 \quad (n_f=3, \quad \Lambda_V^{(0)}=410\ \text{MeV}).$$

III. THE BACKGROUND COUPLING $\tilde{\alpha}_B(R)$ IN COORDINATE SPACE

From the explicit expressions of $\alpha_B^{(n)}(q)$ it is evident that the coupling $\alpha_B^{(n)}(q)$ is well defined at all momenta q^2 if the condition $m_B>\Lambda_V$ is satisfied. Therefore, the Fourier transform can be used to define the static potential in coordinate space over all distances:

$$V_B(r)\equiv -C_F\frac{\tilde{\alpha}_B(r)}{r}=-C_F 4\pi\int\frac{\alpha_B(q)}{q^2}e^{i\mathbf{qr}}\frac{d\mathbf{q}}{(2\pi)^3}. \quad (36)$$

From here a relation similar to Eq. (4) follows:

$$\tilde{\alpha}_B(r)=\frac{2}{\pi}\int_0^\infty dq\frac{\sin qr}{q}\alpha_B(q)=\frac{2}{\pi}\int_0^\infty dx\frac{\sin x}{x}\alpha_B(x/r), \quad (37)$$

where now the background coupling $\alpha_B(x)$ depends on the variable

$$t_B(x)=\ln\frac{x^2+m_B^2r^2}{\Lambda_V^2r^2}. \quad (38)$$

This integral (37) cannot be taken analytically even in the one-loop approximation and was calculated numerically in n-loop approximations ($n=1,2$) with the use of the parameters (25). The behavior of background coupling $\tilde{\alpha}_B^{(2)}(r)$ and $\tilde{\alpha}_B^{(1)}(r)$ is shown in Fig. 2 in the range $0\leqslant r\leqslant 1.4$ fm.

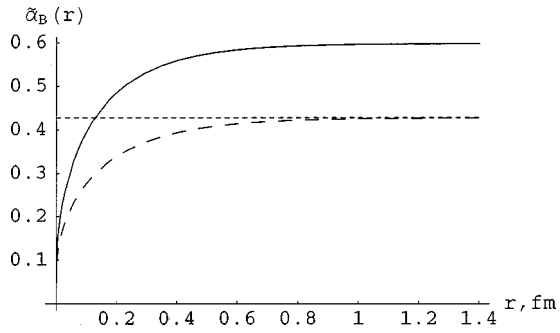

FIG. 2. The one-loop $\tilde{\alpha}_B^{(1)}(r)$ (solid line) and the two-loop $\tilde{\alpha}_B^{(2)}(r)$ (dashed line) background couplings in the quenched approximation; in both cases $\Lambda_V^{(0)}=385$ MeV, $m_B=1.0$ GeV; two-loop asymptotics, $\alpha_{\rm cr}^{(2)}=0.428$, is shown.

From Fig. 2 one can see that two-loop background coupling in coordinate space is approaching the freezing value at relatively short distances, $r\gtrsim 0.4$ fm, and the values of $\tilde{\alpha}_B^{(n)}(r)(n=1,2)$ at the Sommer scale $r_0\approx 0.5$ fm are the following:

$$\tilde{\alpha}_B^{(1)}(r_0=0.5\ \text{fm})=0{,}574; \quad \tilde{\alpha}_B^{(2)}(r_0=0.5\ \text{fm})=0.404. \quad (39)$$

It is of interest to notice that the two-loop coupling at the distance r_0 practically coincides with the number $\alpha=0.39$ widely used in the Cornell potential [1], while the one-loop coupling is too large. The fact that two-loop background coupling is almost constant already at $r\gtrsim 0.4$ fm can be considered as an important argument in favor of the choice $\tilde{\alpha}_B(r)=\text{const}$ in low-energy spectroscopy. In Fig. 3, $\tilde{\alpha}_B^{(2)}(r)$ is shown for two different values of the background mass: $m_B=1.0$ GeV (solid line) and $m_B=1.1$ GeV (dashed line). As seen from Fig. 3, the difference between them is becoming essential already at $r\approx 0.3$ fm, being about 10% over all distances $r>0.3$ fm; their freezing values are $\alpha_{\rm fr}^{(2)}(m_B=1.0\ \text{GeV})=0.428$, $\alpha_{\rm fr}^{(2)}(m_B=1.1\ \text{GeV})=0.382$ (in both cases $\Lambda_V^{(0)}=385$ MeV).

The freezing value in coordinate space turns out to be just the same as in momentum space, i.e., for $n_f=3$ and n_f

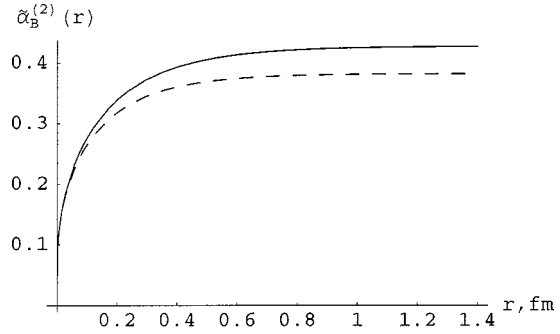

FIG. 3. The background coupling $\tilde{\alpha}_B^{(2)}(r)$ in coordinate space for two values of the background mass m_B: $m_B=1.0$ GeV (solid line) and $m_B=1.1$ GeV (dashed line); in both cases $\Lambda_V^{(0)}=385$ MeV.

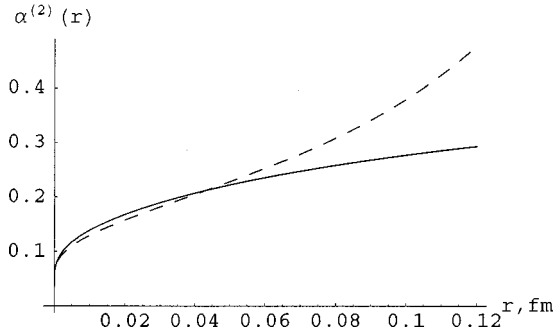

FIG. 4. The background coupling $\tilde{\alpha}_B^{(2)}(r)$ with $\Lambda_V^{(0)}=385$ MeV, $m_B=1.0$ GeV (solid line) compared to the perturbative $\tilde{\alpha}_V^{(2)}(r)$ with $\Lambda_R=686$ MeV (dashed line) at short distances.

$=0$ ($\Lambda_V=385$ MeV) they are given by the numbers from Eq. (35). This property is true also for the phenomenological potential used in Ref. [3]:

$$\alpha_{\rm GI}(q=0)=\alpha_{\rm GI}(r\to\infty)=0.60, \tag{40}$$

since in coordinate space the coupling $\alpha_{\rm GI}(r)$ corresponding to $\alpha_{\rm GI}(q)$ in Eq. (29) is

$$\alpha_{\rm GI}(r)=0.25\Phi(2r)+0.15\Phi(1.581r)+0.20\Phi(15{,}811r), \tag{41}$$

where $\Phi(z)$ is the error function. Thus for three flavors the phenomenological value $\alpha_{\rm fr}\approx 0.6$ was found to be a bit larger than our number $\alpha_{\rm cr}^{(2)}=0.54$ [see Eq. (35) for $n_f=3$].

With $\tilde{\alpha}_B(r)$ calculated above we can compare the background potential $V_B(r)$ (37) to the lattice static potential from Ref. [18]. Here we are mostly interested in the short-range potential, in particular in the influence of background mass m_B on its behavior. The properties of $\tilde{\alpha}_B(r)$ at small r will be considered in the next section.

IV. $\tilde{\alpha}_B(R)$ AT SHORT DISTANCES

Recently very precise lattice measurements of the static potential at short distances were presented [18]. Having these data one has a unique opportunity to compare theoretical predictions about the background coupling and the potential $V_B(r)$ with precise lattice data in the quenched approximation. We remind the reader that our calculations of $\tilde{\alpha}_B^{(n)}(r)$ ($n=1,2$) were done without any arbitrary parameter: $\Lambda_V^{(0)}=385$ MeV ($n_f=0$) was fixed from lattice data [Eq. (14)] and $m_B=1.0$ GeV from the fine-structure splitting of $1P$ and $2P$ states in bottomonium. In Fig. 4, $\tilde{\alpha}_B^{(n)}(r)$ is compared to the perturbative running coupling $\tilde{\alpha}_V^{(2)}(r)$ at $r\leqslant 0.12$ fm, $\tilde{\alpha}_V^{(2)}(r)$ is given by the expression ($r\Lambda_R\ll 1$)

$$\tilde{\alpha}_V^{(2)}(r)=\tilde{\alpha}_V^{(1)}(r)\left\{1-\frac{\beta_1}{\beta_0^2}\frac{\ln y_R}{y_R}\right\} \tag{42}$$

with

TABLE I. The background coupling $\tilde{\alpha}_B^{(2)}(r)$ ($\Lambda_V^{(0)}=385$ MeV, $m_B=1.0$ GeV) compared to perturbative coupling $\tilde{\alpha}_V^{(2)}(r)$ with $\Lambda_R^{(0)}=686$ MeV.

r (fm)	$\tilde{\alpha}_B^{(2)}(r)$	$\tilde{\alpha}_V^{(2)}(r)$	r (fm)	$\tilde{\alpha}_B^{(2)}(r)$	$\tilde{\alpha}_V^{(2)}(r)$
0.002	0.0964	0.0924	0.024	0.1757	0.1667
0.004	0.11095	0.10505	0.030	0.1880	0.1807
0.006	0.1216	0.1209	0.0355	0.1988	0.1943
0.008	0.1303	0.1221	0.041	0.2085	0.2079
0.012	0.1446	0.1352	0.049	0.2204	0.2264
0.016	0.1564	0.1465	0.057	0.2311	0.2455
0.020	0.1666	0.1569	0.063	0.2384	0.2605

$$\tilde{\alpha}_V^{(1)}(r)=\frac{4\pi}{\beta_0 y_R},\qquad y_R=\ln\frac{1}{\Lambda_R^2 r^2}, \tag{43}$$

and we have the following prescription for the value of the QCD constant $\Lambda_R(n_f)$ [24,13]:

$$\Lambda_R^{(n_f)}=\Lambda_V^{(n_f)}\exp\gamma_E\,. \tag{44}$$

In Eq. (44), γ_E is the Euler constant ($\gamma_E=0.5772157$), and in the quenched approximation $\Lambda_V^{(0)}$ is given by the number (14), therefore, for $n_f=0$,

$$\Lambda_R^{(0)}=684\pm 53\ \ {\rm MeV}. \tag{45}$$

In our calculations below we take the number

$$\Lambda_R^{(0)}=686\ \ {\rm MeV}, \tag{46}$$

which corresponds to $\Lambda_V^{(0)}=385$ MeV according to the relation (44).

The numerical comparison of the "exact" background coupling $\tilde{\alpha}_B^{(2)}(r)$ ($\Lambda_V=385$ MeV, $n_f=0$) and the corresponding perturbative $\tilde{\alpha}_V^{(2)}(r)$ with $\Lambda_R^{(0)}$ from Eq. (46) is presented in Table I for the distances in the range

$$0.002\ \ {\rm fm}\leqslant r\leqslant 0.15\ \ {\rm fm}. \tag{47}$$

One can see that the difference between these two couplings,

$$\Delta\alpha_B^{(2)}(r)=\tilde{\alpha}_B^{(2)}(r)-\tilde{\alpha}_V^{(2)}(r)\quad (n=1,2), \tag{48}$$

has several prominent features.

First, at very short distances, $r<0.04$ fm, the correction $\Delta\alpha_B^{(2)}(r)$ is *positive*, i.e.,

$$\tilde{\alpha}_B^{(2)}(r)>\tilde{\alpha}_V^{(2)}(r)\quad (r<0.04\ \ {\rm fm}), \tag{49}$$

and relatively small. It is about 6% at $r=0.02$ fm and still remains $\sim 4\%$ at much smaller $r=0.002$ fm so that $\tilde{\alpha}_B^{(2)}(r)$ approaches the perturbative running coupling $\tilde{\alpha}_V^{(2)}(r)$ rather slowly. In the one-loop approximation this correction was calculated analytically in Ref. [14]:

$$\Delta\alpha_B^{(1)}(r)=\frac{\pi^3}{6\beta_0[-\ln(\Lambda_V r)]^3},\quad |\ln(\Lambda_V r)|\gg 1. \quad (50)$$

It is positive and less than 5% only at very short distances, $r<0.007$ fm. The important feature of $\Delta\alpha_B^{(1)}(r)$ is that it does not depend on the background mass m_B in the limit $r\to 0$.

Secondly, the values of $\tilde{\alpha}_B^{(2)}(r)$ and $\tilde{\alpha}_V^{(2)}(r)$ coincide at the point $r=0.041$ fm, i.e.,

$$\Delta\alpha_B^{(2)}(r=0.041\ \text{fm})=0. \quad (51)$$

At bigger distances, in particular, in the range

$$0.04\ \text{fm}<r\lesssim 0.15\ \text{fm} \quad (52)$$

this correction is *negative and fast growing*, e.g., it is 13% at $r=0.07$ fm, already 36% at $r=0.10$ fm, and reaches 100% at $r=0.14$ fm although all these points lie rather far from the Landau pole, $r_{\text{pole}}=0.29$ fm.

The explanation of why the perturbative coupling is essentially larger than the background coupling at rather small r was given in Ref. [14]. It was shown there that in coordinate space the QCD constant Λ_R can be defined as a constant [given by Eq. (45)] only at very short distances while in the transition region (52) the role of the QCD "constant" plays a function $\tilde{\Lambda}_R(r)$ dependent on the distance:

$$\Lambda_R\to\tilde{\Lambda}_R(r)\cong\Lambda_V\exp\left(\gamma_E+\sum_{k=1}^{\infty}\frac{(-m_B r)^k}{k!k}\right)$$

$$\cong\Lambda_R\exp\left(-m_B r+\frac{1}{4}m_B^2 r^2\right). \quad (53)$$

Then with the use of the function $\tilde{\Lambda}_R(r)$ the perturbative coupling $\tilde{\alpha}_V^{(2)}(r)$ reproduces $\tilde{\alpha}_B^{(2)}(r)$ in the range (52) with an accuracy better than 5%. Actually, this approximation (53) can be used only at distances

$$m_B r-\frac{m_B^2 r^2}{4}<\gamma_E \quad \text{or} \quad r\lesssim 0.15\ \text{fm}. \quad (54)$$

In what follows, the region (54) is called as the *transition region*. By direct calculations of the integral (37) it can be shown that at longer distances $\tilde{\Lambda}_R(r)$ is approaching the vector constant Λ_V [14]:

$$\tilde{\Lambda}_R\to\Lambda_V \quad \text{at} \quad r\gtrsim 0.15\ \text{fm}. \quad (55)$$

V. STATIC INTERQUARK POTENTIAL

Knowing the differences $\Delta\alpha_B^{(n)}(r)\equiv\tilde{\alpha}_B^{(n)}(r)-\tilde{\alpha}_V^{(n)}(r)$ one can calculate the corresponding differences $\Delta V_B^{(n)}(r)$ between the background and perturbative static potentials:

$$\Delta V_B^{(n)}(r)=-\frac{4}{3}\frac{\Delta\alpha_B^{(n)}(r)}{r} \quad (n=1,2). \quad (56)$$

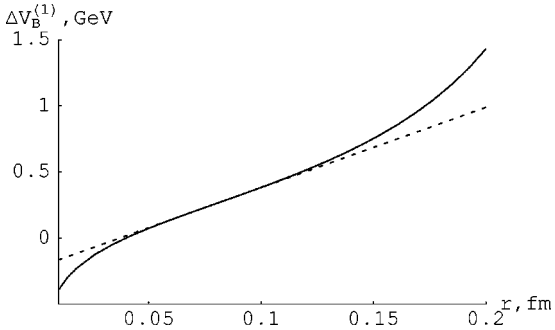

FIG. 5. The difference $\Delta V_B^{(1)}$ between the background and perturbative potentials in the one-loop approximation (solid line). The tangent with the slope $\sigma_B^{*(1)}=1.20$ GeV^2 is shown by the dashed line. The parameters are the same as in Fig. 4

Numerically calculated $\Delta V_B^{(1,2)}(r)$ are shown in Figs. 5 and 6 correspondingly. We observe the linear rise of potentials illustrated by the tangents (dashed lines). Tangent slopes $\sigma_B^{(n)}(r)$ are defined as

$$\sigma_B^{*(n)}(r)=\frac{\partial\Delta V_B^{(n)}(r)}{\partial r}. \quad (57)$$

We see from the figures that

$$\sigma_B^{*(1)}=1.20\ \text{GeV}^2, \quad 0.05\ \text{fm}<r<0.12\ \text{fm}, \quad (58)$$

$$\sigma_B^{*(2)}=0.87\ \text{GeV}^2, \quad 0.03\ \text{fm}<r<0.09\ \text{fm}. \quad (59)$$

This large difference means that the perturbative $\tilde{\alpha}_V(r)$ fails to describe lattice data in this region. Nevertheless, we try here to compare our results (58) and (59) with the lattice ones from Ref. [18]. After perturbative potential subtraction from the lattice static quenched potential, lattice data in the region $0.03\ \text{fm}<r<0.15$ fm were parametrized by the linear potential with the slope

$$\sigma_{\text{lat}}^*=(1.20\pm 0.36)\ \text{GeV}^2, \quad 0.03\ \text{fm}<r<0.15\ \text{fm}. \quad (60)$$

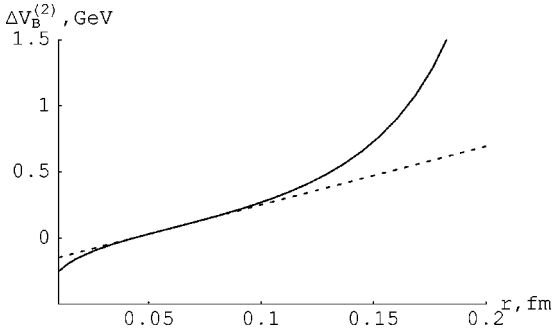

FIG. 6. The difference $\Delta V_B^{(2)}$ between the background and perturbative potentials in the two-loop approximation (solid line). The tangent with the slope $\sigma_B^{*(2)}=0.87$ GeV^2 is shown by the dashed line. The parameters are the same as in Fig. 4

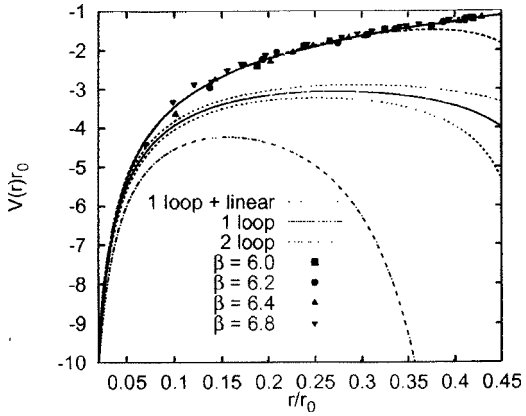

FIG. 7. The static potential $V(r)=V_B^{(2)}(r)+\sigma r+C$ with the parameters of $V_B^{(2)}(r)$ from Fig. 4, $\sigma=0.2$ GeV^2 and $C=-253$ MeV (solid line, imposed on lattice points) comparatively to the lattice static potential from Ref. [18]; Sommer scale $r_0=2.5$ GeV^{-1}. The one-loop and two-loop perturbative potentials from Ref. [18] (see Sec. V) are shown by a thin solid line below the lattice points and a dash-dotted line, respectively; one-loop + linear $\sigma^*_{\rm lat}r$ potential ($\sigma^*_{\rm lat}=1.20$ GeV) is shown by a dashed line.

One can see that $\sigma^*_{\rm lat}$ corresponds to $\sigma_B^{*(1,2)}$ within one standard error. We conclude that this large linear slope of potential is well explained using $\alpha_B(r)$ instead of $\widetilde{\alpha}_V(r)$. In Fig. 7, we compare the lattice static potential from Ref. [18] at the distances $0.05<r/r_0<0.45$ with the potential

$$V(r)=-\frac{4}{3}\frac{\alpha_B^{(2)}(r)}{r}+\sigma r+C, \tag{61}$$

where $\sigma=0.2$ GeV^2 and $C=-253$ MeV (shown by a solid line). This potential includes the background perturbative potential $V_B^{(2)}(r)$ and the linear confining potential σr. The constant C corresponds to the quark self-energy. We observe that this potential describes all lattice data remarkably well.

In Fig. 7, *one-loop* and *two-loop perturbative potentials*, calculated in Ref. [18], are also shown. The difference between them and lattice points is large and explained above. The *one-loop perturbative + linear potential* with the slope $\sigma^*_{\rm lat}$ is also shown. It describes lattice points up to $r/r_0=0.35$, but fails to describe the rest of the data because of the Landau pole of $\widetilde{\alpha}_V(r)$. On the contrary, $V(r)$ [Eq. (61)] not only describes all the lattice data presented in Fig. 7 in the region $0.05<r/r_0<0.3$, but also all the lattice data available up to $r=3r_0$ with a reasonable accuracy.

What is the physics of the linear part of $V(r)$? In the framework of BPT [27] it was shown that the linear confining potential starts from the quark distances close to the gluonic correlation length T_g. From the lattice data, $T_g\approx0.2$ fm [28] and $T_g=0.12-0.15$ fm [29]. At smaller distances one needs to take into account an interference of perturbative and nonperturbative effects [30]. As was shown in Ref. [30], the interference potential at $r\lesssim T_g$ behaves like a linear one with the slope about σ, while the nonperturbative potential is proportional to r^2 and small in this region [27]. At distances $r\gtrsim T_g$, the interference interaction vanishes, while the nonperturbative potential becomes the linear one with the same slope σ. As a result, the sum of these potentials may be close to a linear one with the standard slope σ over all distances. This linear behavior of nonperturbative potential at short distances is important for the fine-structure fit in charmonium [10]. Note also that the linear potential $V^{(\rm NP)}(r)$ is consistent with the ''short string'' potential generated either by the topologically defined pointlike monopoles or infinitely thin P vortices within the Abelian Higgs model [31]. The distinguishing feature of the last potential is that it does not change its slope at all distances. We leave the detailed numerical analysis of this effect to a subsequent paper.

VI. CONCLUSIONS

In our paper, the strong coupling $\widetilde{\alpha}_B(r)$ in coordinate space, deduced in BPT, is investigated and the corresponding perturbative potential is compared to the short-range lattice static potential from Ref. [18]. The following prominent features of $\widetilde{\alpha}_B(r)$ are observed.

(i) The background coupling attains the asymptotics of standard perturbative coupling $\widetilde{\alpha}_V(r)$ only at very short distances, $r<0.04$ fm, where the QCD constant $\Lambda_R=\Lambda_V\exp\gamma_E$, and Λ_V, the QCD constant in the ''V-scheme,'' is considered to be a well established number in the quenched approximation.

(ii) At larger r, a function $\widetilde{\Lambda}_R(r)$ plays the role of the QCD constant, which at short distances, $m_Br<\gamma_E$, is approximately given by

$$\widetilde{\Lambda}_R(r)\approx\Lambda_R\exp\left(-m_Br+\frac{m_B^2r^2}{4}\right), \tag{62}$$

where $m_B=1.0$ GeV is the background mass fixed by fit to fine-structure splittings of $1P$ and $2P$ levels in bottomonium. In fact the condition

$$m_Br-\frac{1}{4}m_B^2r^2\leqslant\gamma_E \tag{63}$$

defines the narrow transition region: 0.05 fm$\leqslant r\leqslant$0.15 fm, where $\widetilde{\Lambda}_R(r)$ decreases almost twice, from the value Λ_R at $r\approx0.05$ fm to the number close to Λ_V at $r=0.15$ fm.

(iii) The static potential $V_B(r)$ in BPT, defined through $\widetilde{\alpha}_B(r)$ in the usual way, Eq. (36), is in good agreement with the quenched lattice static potential measured at short distances [18].

(iv) The specific behavior of $\widetilde{\alpha}_B(r)$ in the transition region produces a linear rise of the difference $\Delta V(r)=V_B(r)-V_P(r)$ with the slope $\sigma^*\sim1$ GeV^2 in accordance with the lattice data. Moreover, we have obtained a very good agreement with the lattice data using the sum $V_B(r)+\sigma r$ with $\sigma=0.2$ GeV^2.

(v) At distances $r\gtrsim0.2$ fm, the function $\widetilde{\Lambda}_R(r)$ turns out to be almost constant; $\widetilde{\Lambda}_R(r)\approx\Lambda_V$ over all distances, so that

at $r>0.3$ fm the coupling $\tilde{\alpha}_B(r)$ fast approaches the freezing value $\tilde{\alpha}_B(\infty)$. This fact helps us to understand why the use of $\tilde{\alpha}_V(r)=\text{const}$ in the static potential of the quark model [3] appears to be a good approximation in hadron spectroscopy.

(vi) The freezing value of the background coupling coincides in momentum and coordinate space, and this statement can be checked in different processes in low-energy QCD. Our estimate for α_{fr} is 0.53–0.60.

ACKNOWLEDGMENTS

The authors are grateful to Yu. A. Simonov for many fruitful discussions. This work has been supported by RFFI Grant No. 00-02-17836.

[1] E. Eichten *et al.*, Phys. Rev. Lett. **34**, 369 (1975); Phys. Rev. D **21**, 203 (1980).
[2] J.L. Richardson, Phys. Lett. **82B**, 272 (1979).
[3] S. Godfrey and N. Isgur, Phys. Rev. D **32**, 189 (1985).
[4] A.C. Mattingly and P.M. Stevenson, Phys. Rev. D **49**, 437 (1994).
[5] A.M. Badalian, Yad. Fiz. **60**, 1122 (1997) [Phys. At. Nucl. **60**, 1003 (1997)].
[6] Yu.L. Dokshitzer, V.A. Khose, and S.I. Troyan, Phys. Rev. D **53**, 89 (1996); Yu.L. Dokshitzer, hep-ph/9812252.
[7] Yu.A. Simonov, *Perturbative QCD in the Nonperturbative QCD Vacuum*, Proceeding of Schladming Winter School, 1996 (Springer, Berlin, 1997), Vol. 479, p. 139; Pis'ma Zh. Eksp. Teor. Fiz. **57**, 513 (1993); Yad. Fiz. **58**, 113 (1995).
[8] A.M. Badalian and Yu.A. Simonov, Yad. Fiz. **60**, 714 (1997) [Phys. At. Nucl. **60**, 630 (1997)].
[9] D.V. Shirkov and I.L. Solovtsov, Phys. Rev. Lett. **79**, 1209 (1997); D.V. Shirkov, Nucl. Phys. B (Proc. Suppl.) **64**, 106 (1998); JINR Report No. R2-2001-153, hep-ph/0107282.
[10] A.M. Badalian and V.L. Morgunov, Phys. Rev. D **60**, 116008 (1999); Yad. Fiz. **62**, 1086 (1999) [Phys. At. Nucl. **62**, 1019 (1999)].
[11] A.M. Badalian and B.L.G. Bakker, Phys. Rev. D **62**, 094031 (2000).
[12] Yu.S. Kalashnikova, A.V. Nefediev, and Yu.A. Simonov, Phys. Rev. D **64**, 014037 (2001).
[13] M. Jezabek, M. Peter, and Y. Sumino, Phys. Lett. B **428**, 352 (1998).
[14] A.M. Badalian, Yad. Fiz. **63**, 2269 (2000) [Phys. At. Nucl. **63**, 2173 (2000)].
[15] S.P. Booth *et al.*, Phys. Lett. B **294**, 385 (1992); K.D. Born, E. Laermann, T.F. Walsh and P.M. Zerwas, *ibid.* **329**, 325 (1994).
[16] G.S. Bali and K. Schilling, Phys. Rev. D **47**, 661 (1993); G.S. Bali, K. Schilling, and A. Wachter, *ibid.* **56**, 2566 (1997).
[17] SESAM Collaboration, U. Glässner *et al.*, Phys. Lett. B **383**, 98 (1996); C. Bernard *et al.*, Phys. Rev. D **62**, 034503 (2000).
[18] G.S. Bali, Phys. Lett. B **460**, 170 (1999).
[19] S. Capitani, M. Lüscher, R. Sommer, and H. Witting, Nucl. Phys. **B544**, 669 (1999).
[20] M. Peter, Phys. Rev. Lett. **78**, 602 (1997); Nucl. Phys. **B501**, 471 (1997).
[21] Y. Schröder, Phys. Lett. B **447**, 321 (1999)
[22] Yu.A. Simonov, Yad. Fiz. **58**, 113 (1995).
[23] G. Parisi and R. Petronzio, Phys. Lett. **94B**, 51 (1980); J.M. Cornwall, Phys. Rev. D **26**, 1453 (1982).
[24] A. Billoire, Phys. Lett. **92B**, 343 (1980).
[25] Particle Data Group, D. Groom *et al.*, Eur. Phys. J. C **15**, 85 (2000).
[26] F.J. Yndurain, QCD: Perturbative or nonperturbative?, 1997, Lisbon, 1999.
[27] Yu.A. Simonov, Nucl. Phys. **B307**, 512 (1988); A.M. Badalian and V.P. Yurov, Yad. Fiz. **56**, 55 (1993) [Phys. At. Nucl. **56**, 175 (1993)]; A.M. Badalian and Yu.A. Simonov, *ibid.* **59**, 2247 (1996) [**59**, 2164 (1996)].
[28] A.Di. Giacomo and H. Panagopoulos, Phys. Lett. B **285**, 133 (1992).
[29] G. Bali, N. Bramilla, and A. Vairo, Phys. Lett. B **421**, 265 (1998).
[30] Yu.A. Simonov, Phys. Rep. **320**, 265 (1999).
[31] V.I. Zakharov, lecture given at the Winter School of physics of ITEP, 1999; M.N. Chernodub, F.V. Gubarev, M.V. Polikarpov, and V.I. Zakharov, Phys. Lett. B **475**, 303 (2000).